p-InAsSbP/n^0-InAs/n^+-InAs photodiodes for operation at moderate cooling (150−220 K)

© P.N. Brunkov[+], N.D. Il'inskaya[+], S.A. Karandashev[+], N.M. Latnikova[∗], A.A. Lavrov[+]
B.A. Matveev[+,¶], A.S. Petrov[≠], M.A. Remennyi[+], E.N. Sevostyanov[∗], N.M. Stus[+]

[+] Ioffe Physicotechnical Institute, Russian Academy of Sciences,
194021 St. Petersburg, Russia
[∗] LETI Ul'yanov (Lenin) St. Petersburg Electrotechnical University,
197376 St. Petersburg, Russia
[≠] 194223 St. Petersburg, Russia

InAs single heterostructure photodiodes were considered as alternatives to cooled CdHgTe-based detectors sensitive to radiation around $3\,\mu$m spectral region in a wide temperature range 77−300 K. Estimations of detectivity as well as $p-n$ junction position in InAs heterostructures have been obtained via photoelectrical and AFM measurements.

1. Introduction

InAs based photodiodes (PDs) operate in the first atmospheric window and promise considerable advantages over other types of photodetectors in a variety of applications including pyrometry [1], gas analysis [2] and thermovoltaic energy production [3,4]. In [5,6] an additional broad band gap p-InAs$_{1-x-y}$Sb$_x$P$_y$ „window" layer with $y \approx 2.2x$ was suggested for performance improvements in InAs PDs operating at temperatures below 300 K. The above improvements were later confirmed in a number of theoretical and experimental papers devoted to single (SH) [1–4,7–12] and double heterostructure (DH) [9,13] PDs with p-type InAsSbP claddings and n-InAs active layers operating in a wide temperature range (77−350 K). Nowadays several companies are trying to introduce the above PDs with backside and front surface illumination operation modes to the market. On the other hand there are still very limited data on photoelectrical properites of a p-InAsSbP/n-InAs heterojunction as most known devices do not contain the above junction, instead the $p-n$ junction position in many published devices did not coincide with the InAsSbP/InAs interface. The latter was thought to be a consequence of an acceptor impurity diffusion during the growth process (see, e.g. [11]) with the result that a $5-15\,\mu$m thick p-InAs layer was sandwiched between p-InAsSbP and n-InAs semiconductors with no real chance for attributing these samples to the „p-InAsSbP/n-InAs structures". In fact, most known devices are based on the isotype p-InAsSbP/p-InAs junctions. Moreover, in most cases [3–8,11] experimental specimens contained the only p-InAsSbP epitaxial layer with the active area formed inside the Chokhralski grown InAs substrate. Commercial undoped n-InAs substrates contain $n \approx 2 \cdot 10^{16}\,\text{cm}^{-3}$ free electrons and this decreases the possibility of thorough selection of process parameters for producing a PD active area with a required thickness and doping. For example, epitaxial growth from a gadolinium doped melt onto n-InAs ($n = 2 \cdot 10^{16}\,\text{cm}^{-3}$) enables one

reducing the above number down to $5 \cdot 10^{15}\,\text{cm}^{-3}$ in InAs-like active layers [14].

Here we present data on SH PDs with two epitaxial layers, namely p-InAsSbP and n^0-InAs, grown onto a n^+-InAs substrate. In addition to our previous findings [12] emphasis is made on PD performance for operation at moderate cooling (150−220 K) and at low currents — conditions important for applications where high detectivity (D^*) as well as size and weight of the cooling system are critical. Validation for the use of designation „p-InAsSbP/n-InAs/n^+-InAs photodiodes" in the paper title is also provided.

2. Experimental technique and samples

Lattice matched to InAs epitaxial structures were similar to those we studied previously [9,12] and they contained a heavily doped n^+-InAs (100) substrate ($n^+ \sim 10^{18}\,\text{cm}^{-3}$), an undoped n-InAs active layer $4-6\,\mu$m thick, and wide energy gap layer („window") of p-InAsSbP$_{0.18}$(Zn) (band gap $E_g = 440$ meV) solid solution $2-3\,\mu$m thick. The energy gap discontinuities at the type II heterointerface were $\Delta E_c = 120$ meV (conduction band) and $\Delta E_v = -30$ meV (valence band) at 300 K; the corresponding band scheme can be found in [15]. PD chips had a $330 \times 330\,\mu$m square mesa produced by IoffeLED company using standard photolithography and „wet" etching processes. A disc anode contact with a diameter of $D_a = 80\,\mu$m was formed in the center of the mesa onto p-InAsSbP front surface by a sequential thermal evaporation of metals and further electrochemical deposition of gold. A broad cathode contact was formed onto n^+-InAs substrate in a similar to the above manner and occupied the entire area of the chip backside. The sensitivity and spectral characteristics of the obtained front surface illuminated (FSI) PDs were measured using a black-body model heated up to 573 K.

The thickness of the p-InAsSbP layer was estimated by imaging of the $(1\bar{1}0)$ cleaved plane in the back scattered
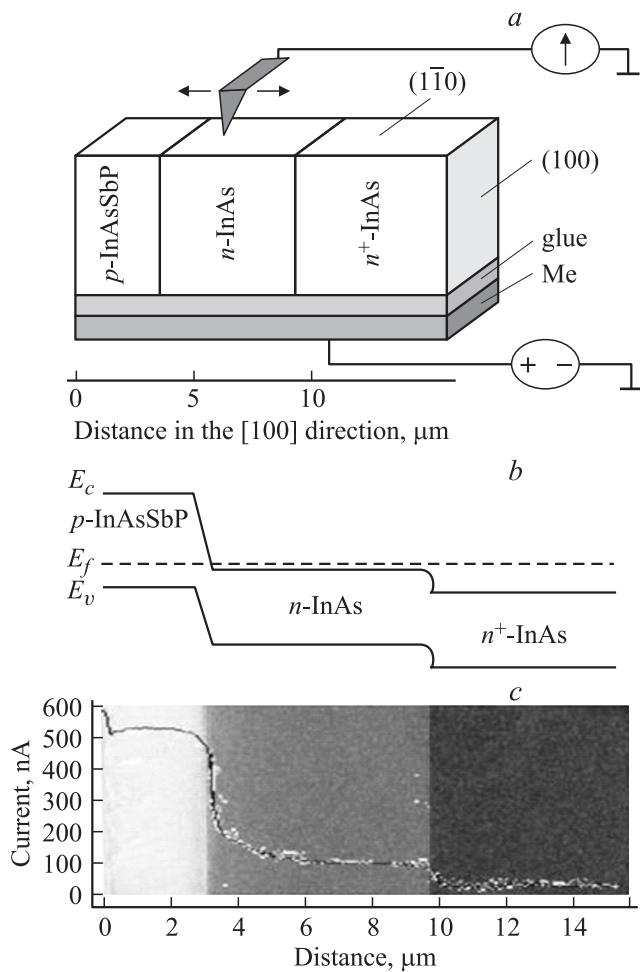
¶ E-mail: bmat@iropt3.ioffe.ru

Figure 1. Schematic image of the measurement set up (*a*), energy band diagram of the PD (*b*) and current vs cantilever position at $V_{DC} = 3$ mV bias voltage as one dimensional (curve) and two dimensional SSRM image of the $(1\bar{1}0)$ cleaved plane (*c*).

investigation as this is the first evidence for coincidence of the above junctions in InAsSbP/InAs based structures.

3. Experimental results and discussions

Fig. 2 presents typical current sensitivity spectra $S_I(\lambda)$ measured at 77, ~ 120 and 295 K while *p*-side of the PD was illuminated by a Globar as schematically shown in the insert to the figure. The sensitivity spectrum at room temperature is relatively broad due to its short wavelength shoulder and is typical for the FSI InAs PDs including those available at the market. The longwave cut-off of the spectrum shifts is in accordance with temperature variation of the energy gap while change of the shortwave shoulder reflects temperature dependence of both nonequilibrium carrier diffusion towards $p-n$ junction and radiation propagation through *p*-InAsSbP. The peak PD sensitivity value exhibited weak dependence on temperature variation amounting to 1.1 and 1 A/W at 77 and 300 K, respectively.

As seen from Fig. 3 reverse current had well pronounced saturation at temperatures close to 300 K; this positive performance change probably originates from the use of epitaxial *n*-InAs active layer instead of the bulk substrate material. Previous *p*-InAsSbP/*n*-InAs PDs with active layer formed in the body of the substrate exhibited soft breakdown attributed to trap assisted tunneling [6] or avalanche amplification [11] in a wide temperature range including room temperature.

In the temperature range of $160 < T < 220$ K the forward current had well pronounced tendency to vary as $\exp(eU/\beta kT)$ where U is the bias voltage, β is the ideality factor, k is the Boltzmann constant and T is the temperature (see the solid and dashed lines in Fig. 3 presenting exponents corresponding to different T and β values). At room temperature forward current did not follow the above exponent evidently due to low dynamical

electron mode (BSE) sensitive to semiconductor composition constituted to $2.3\,\mu$m. The latter value was close to our estimations made through the use of an optical microscope while the thickness of a transition zone at the *p*-InAsSbP/*n*-InAs interface did not exceed $0.3\,\mu$m. We also measured spreading resistance together with spatial relief along the [111] direction onto the $(1\bar{1}0)$ plane using a cleaved sample glued by a conductive glue onto a conductive header (Me) as was suggested in [16] and is shown in Fig. 1, *a*. Inspection of the scanning spreading resistance microscopy (SSRM) image recorded at the voltage $V_{DC} = 3$ mV revealed three regions with sufficiently different impurity concentrations that corresponded to the substrate and two epitaxial layers as seen from comparison of curve presenting photodetector signal vs distance and cleaved $(1\bar{1}0)$ plane image in Fig. 1, *c*. It can be concluded from data in Fig. 1, *c* that within the set up accuracy the InAsSbP/InAs interface and $p-n$ junction location coincide. This is a distinguishing feature of the samples under
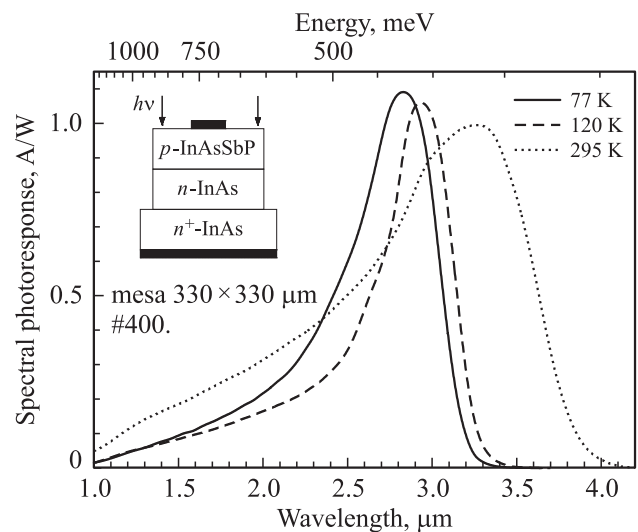

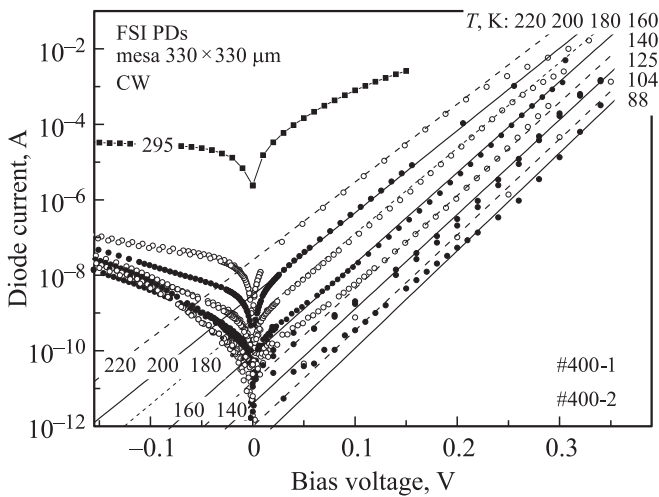**Figure 2.** Current sensitivity spectra, $S_I(\lambda)$, in InAs SH PD at 77, 120 and 295 K.

Figure 3. Current–voltage characteristics of InAs SH PD at 88, 104, 125, 140, 160, 180, 200 and 220 K.

$p-n$ junction resistance accompanied by a current crowding under small area anode — a feature of structures with high resistance (p-InAsSbP) contact layer [15]. The above current–voltage characteristic distortion prevents correct determination of the ideality factor at 300 K; no attempts have been undertaken to extract undistorted data and thus the corresponding value of β was omitted in further considerations. At low forward bias ($3kT/e < U < 0.1$ V) and at temperatures $T < 160$ K a leakage current dominated, while at high bias ($U > 0.1$ V) a diffusion in the neutral areas and generation–recombination in the active layer governs the current. It is usually assumed that stability of a reverse current at small bias against temperature variation indicates tunneling of charge carriers through a narrow band gap $p-n$ junction [17,18]. In our case reverse current exhibits strong temperature dependence, say at $U = -0.01$ V, and thus we are inclined to believe that tunneling (accompanied by high β values, $\beta \gg 2$) is not important in our PDs. The conclusion is also supported by low β values ($\beta < 2.2$) derived at several temperatures from superposition of the „high bias" data in Fig. 3 and $I = I_0[\exp(eU/\beta kT) - 1]$ equation (see data presented in Fig. 4 together with the saturation current I_0 and „old" data from [12]).

As seen from Fig. 4 the total current at high bias is of the diffusion origin at 300 K and is of the generation–recombination one at $T < 120$ K. It follows from the comparison of the above values and the values measured earlier [12] (Fig. 4) that InAs SH PDs performance was underestimated in our previous work as the saturation current and the ideality factor values appeared to be smaller than in [12] obviously due to better measurement accuracy in the current research. The detectivity value at room temperature determined as $D^* = S_I(R_0A/4kT\Delta f)^{0.5}$, $R_0 = \beta kT/I_0$ (see Fig. 5) appeared somewhat smaller than that for the InAs SH and DH backside-illuminated PDs [9], but was higher than the simulated values in [10]. We are

aware that the low temperature D^* values ($T < 160$ K) in Fig. 5 simulated using the above approach were somewhat exaggerated — in fact the leakage current at small bias (see Fig. 3) adds to total noise and reduces D^*. This is not the case for temperatures > 180 K as diffusion current dominates and thus the D^* values reflect real PD performance in a photovoltaic mode of operation. It is also worth mentioning that introduction of the epi-taxially grown n-InAs active layer instead of an active zone in InAs substrate resulted in sufficient dark current reduction, e.g. from $3 \cdot 10^{-6}$ A at $U = -0.1$ V and $T \approx 200$ K in p-InAsSbP/n-InAs PDs [6] down to $2 \cdot 10^{-8}$ A
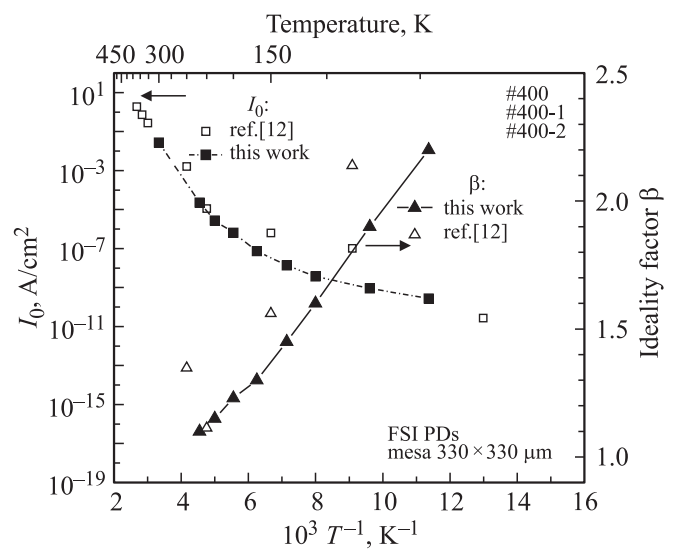

Figure 4. Saturation current I_0 (left scale) and ideality factor β (right scale) for InAs SH PD vs reverse temperature. Data from [12] and our results.
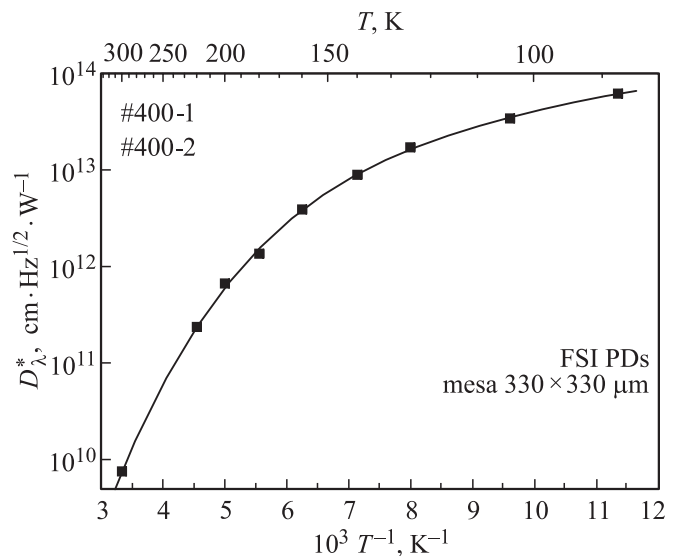

Figure 5. Detectivity at spectrum maximum D^*_λ vs reverse temperature in InAs SH PD. Estimations are made at an assumption $S_I = 1$ A/W.

in *p*-InAsSbP/*n*-InAs/*n*⁺-InAs PDs (see Fig. 3). Due to coincidence of *p−n* junction position and InAsSbP/InAs interface mentioned earlier it is believed that at least part of the space charge region in our PDs is located in a „wide band" InAsSbP quaternary alloy with the result that at low temperatures the total generation−recombination current is smaller than in „narrow band" InAs *p−n* homojunctions. Indeed as follows from data in Fig. 5 the D^* value in our InAs SH PD amounts to $1.4 \cdot 10^{12}\,\mathrm{cm \cdot Hz^{1/2} \cdot W^{-1}}$ at 180 K which is an order of magnitude higher than that in the homojunction *p*-InAs/*n*-InAs PDs at 180 K [19] and three fold higher than that in the *p*-InAsSbP/*p*-InAs/*n*-InAs heterostructure PDs at 77 K [11].

4.   Conclusions

Single heterojunction PDs on the base of *p*-InAsSbP/ *n*-InAs with peak sensitivity in the 2.8−3.4 µm wavelength range demonstrated both diffusion and recombination−generation of carriers that determined the current at room and low temperatures, respectively. At the liquid nitrogen and moderate cryogenic temperatures (150−200 K) these PDs showed superior performance in terms of R_0 and D^* values with respect to their analogs containing a *p*-InAs/*n*-InAs homojunction. At the temperature of $T = 180$ K comfortable for cooling systems the D^* value amounted to suitable for sensing application value of $1.4 \cdot 10^{12}\,\mathrm{cm \cdot Hz^{1/2} \cdot W^{-1}}$.

References

[1] G.Yu. Sotnikova, S.E. Aleksandrov, G.A. Gavrilov. Proc. SPIE, **8073**, 80731D (2011); DOI: 10.1117/12.886309.

[2] A.A. Kuznetsov, O.B. Balashov, E.V. Vasil'ev, S.A. Loginov, A.I. Lugovskoi, E.Ya. Cherniak. Prib. Sist. Upravlenie, Kontrol', Diagnostika, N 6, 55 (2003) (in Russian).

[3] M.G. Mauk, V.M. Andreev. Semicond. Sci. Technol., **18** (5), S191 (2003).

[4] V.A. Gevorkyan, V.M. Aroutiounian, K.M. Gambaryan, M.S. Kazaryan, K.J. Touryan, M.W. Wanlass. Thin Sol. Films, **451−452**, 124 (2004).

[5] A.V. Pentsov, S.V. Slobodchikov, N.M. Stus', G.M. Filaretova. USSR Inventor's Certificate N 295951 (1988).

[6] V.V. Tetyorkin, A.V. Sukach, S.V. Stariy, N.V. Zotova, S.A. Karandashev, B.A. Matveev, N.M. Stus. Proc. SPIE, **5957**, 59570Z, (2005); DOI: 10.1117/12.622181.

[7] N.V. Zotova, S.A. Karandashev, B.A. Matveev, A.V. Pentsov, S.V. Slobodchikov, N.N. Smirnova, N.M. Stus', G.N. Talalakin, I.I. Markov. Proc. SPIE, **1587**, 334 (1992); doi: 10.1117/12.56559.

[8] X.Y. Gong, T. Yamaguchi, H. Kan, T. Makino, T. Iida, T. Kato, M. Aoyama, Y. Hayakawa, M. Kumagawa. J. Appl. Phys., **36**, 2614 (1997).

[9] B.A. Matveev, N.V. Zotova, S.A. Karandashev, M.A. Remennyi, N.M. Stus', G.N. Talalakin. SPIE, **4650**, 173 (2002).

[10] R.K. Lal, P. Chakrabarti. Optical. Quantum Electron., **36**, 935 (2004).

[11] M. Ahmetoglu (Afrailov). Infr. Phys. Technol., **53** (1), 29 (2010).

[12] N.D. Il'inskaya, S.A. Karandashev, N.M. Latnikova, A.A. Lavrov, B.A. Matveev, A.S. Petrov, M.A. Remennyi, E.N. Sevost'yanov, N.M. Stus'. Techn. Phys. Lett., **39** (9), 818 (2013).

[13] P.N. Brunkov, N.D. Il'inskaya, S.A. Karandashev, A.A. Lavrov, B.A. Matveev, M.A. Remennyy, N.M. Stus', A.A. Usikova. Infr. Phys. Technol., (2014) in print.

[14] N.V. Zotova, S.A. Karandashov, B.A. Matveev, M.A. Remennyi, N.M. Stus', G.N. Talalakin. Semiconductors, **33** (8), 920 (1999).

[15] N.V. Zotova, S.A. Karandashov, B.A. Matveev, M.A. Remennyy, A.Yu. Rybal'chenko, N.M. Stus'. Semiconductors, **45** (4), 543 (2011); DOI: 10.1134/S1063782611040245.

[16] S.B. Kuntze, D. Ban, E.H. Sargent. Critical Rev. in Sol. St. Mater. Sci., N 30, 71 (2005).

[17] C.H. Kuan, R.M. Lin, S.F. Tang, T.P. Sun. J. Appl. Phys., **80** (9), 5454 (1996); DOI: 10.1063/1.362734.

[18] A. Krier, H.H. Gao, Y. Mao. Semicond. Sci. Technol., **13**, 950 (1998), PII: S0268-1242(98)91383-9.

[19] P.J. Ker, A.R.J. Marchall, J.P.R. David, C.H. Tan, Phys. Status Solidi C, **9**, 310 (2012); DOI: 10.1002/pssb.201100277.

Редактор Л.В. Шаронова